

## BI-STATE CONTROL OF A DUFFING MICRORESONATOR ON THE FALLING EDGE OF THE INSTABILITY

Congzhong Guo<sup>1</sup> and Gary K. Fedder<sup>1,2,3</sup>

<sup>1</sup>Department of Electrical and Computer Engineering,

<sup>2</sup>Institute for Complex Engineered Systems, <sup>3</sup>The Robotics Institute  
Carnegie Mellon University, Pittsburgh, Pennsylvania, USA

### ABSTRACT

This work is the first investigation of a bi-state control technique capable of servoing on the falling edge of the microelectromechanical Duffing resonant bifurcation setpoint. The Duffing microresonator, fabricated in an SOI-MEMS process, features a sharp jump in oscillation amplitude at the bifurcation and is, therefore, ideal for ultrasensitive detection of mass or stress shifts that modify the resonance frequency and hence the jump frequency. The resonator “instability tongue” is characterized to identify the bifurcation points as a function of drive gain. The control system states are set through the AC drive gain while operating at a fixed drive frequency such that one of the system states is within this instability tongue whereas the second state resides outside of this tongue. The amplitude servo point is chosen at the maximum “on” amplitude prior to the jump event. The states are driven by 300 kHz pulse width modulation that is set much faster than the amplitude response dynamics and inhibits the system from latching off as would happen in static operation.

### KEYWORDS

Duffing resonance, Nonlinear control, Bifurcation, Bi-state, Nonlinear resonator, Hysteresis, Recapture, Nonlinear dynamics

### INTRODUCTION

Duffing resonance featuring bifurcation behavior is capable of gauging small resonance changes. These variations in the resonator characteristics are generally modified by the resonant mass or suspension spring stiffness. By probing the shifts in the bifurcation point, sensitive gravimetric and stress detectors can be built. Bifurcation-based detectors provide an ultrasensitive approach to reveal these small changes if a control approach is designed to servo at the bifurcation point. However, the system exhibiting bifurcation behavior is difficult to control because of the slow time manifold the system trajectory has to travel before the bifurcation [1]. The nonlinear system also suffers from hysteresis [2]-[3] due to the necessary nonlinearity in the device. These two artifacts render the classical control possibilities difficult to implement. One analog control scheme at the onset of the bifurcation by [4] is to observe the variance of the signal phase and keep the amplitude very small to avoid the bifurcation jump event such that the long settling time and hysteresis are avoided. Its implementation in a field-programmable gate array to observe the phase statistics limits its on-chip integration. An improved controller with vibration amplitude as the controlled

variable is reported in [5]. The technique settles at relatively small amplitude of below 1.5 nm, with a low signal-to-noise ratio (SNR), making it unsuitable for robust control applications.

This paper proposes a bi-state servo of a MEMS Duffing resonator that controls on the maximum amplitude “on” point prior to the bifurcation jump. In addition to addressing the issues of limit cycling and instability, this new approach also achieves a high SNR with much higher controlled amplitude (e.g., 4.8  $\mu\text{m}$ ).

### DEVICE

Shown in Figure 1 is the 15  $\mu\text{m}$ -thick SOI-MEMS Duffing resonator reported in [6] as the control plant, with a perspective view of the lateral capacitive comb electrode geometry. The capacitive combs are symmetrically placed on both sides of the shuttle mass; the left set serves as the drive electrode and the right set serves as the capacitive pick-off sense electrode. The perforated shuttle mass is suspended by four symmetric crab-leg springs. The nonlinearity inherent in the system stems from the suspension and the electrostatic spring constants from the comb drive.

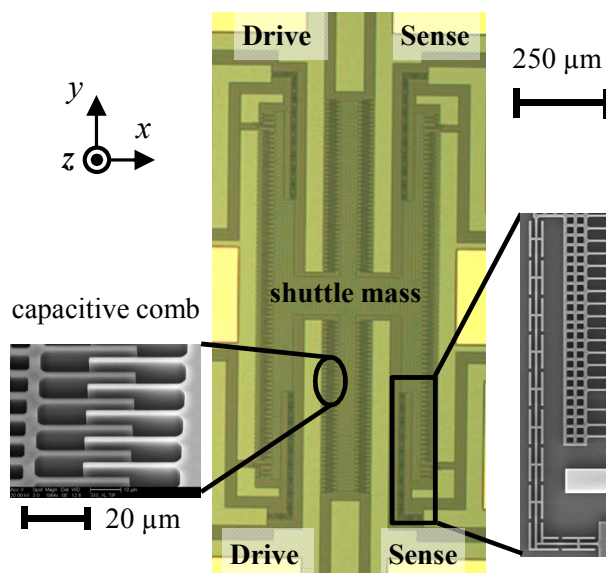


Figure 1: Optical microscope image of the Duffing microresonator with zoomed-in SEM views of the drive comb and the crab-leg spring.

### DUFFING RESONANCE

The typical measured frequency response of the Duffing resonator is plotted in Figure 2. This class of nonlinear resonator exhibits a hysteresis effect when the frequency is swept bi-directionally. The polarization

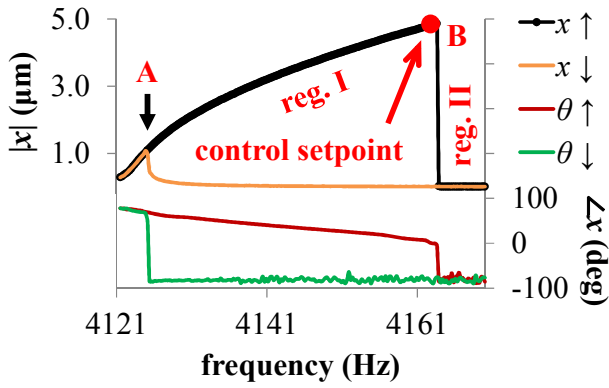


Figure 2: Hysteresis of the Duffing resonator at  $V_{dc,set} = 10\text{ V}$  and  $V_{ac} = 25\text{ mV}$ .  $\uparrow$  symbolizes the frequency up-sweep;  $\downarrow$  is the frequency down-sweep.

voltage on the moving shuttle mass is  $V_{dc,set} = 10\text{ V}$  and the AC sinusoidal drive on the lateral capacitive comb rotor is  $V_{ac} = 25\text{ mV}$ . The test is performed in a vacuum of 25 mTorr. Unlike the harmonic resonator, the resonance peak bends to the right, yielding multi-valued solutions for one frequency value around the resonance. On the edge of the bent peak (point B), a jump in the resonance amplitude from 4.8  $\mu\text{m}$  to 0  $\mu\text{m}$  occurs. The frequency at which the instantaneous jump occurs is called the “bifurcation frequency”  $f_B$ , which equals 4167 Hz for the setpoint B in Figure 2. For a reverse frequency sweep, the jump happens at a lower frequency from 0  $\mu\text{m}$  to 1.0  $\mu\text{m}$  (point A), indicative of hysteresis effect. The region I between points A and B defines the region where a large amplitude response occurs. To the right of point B (region II), the resonance amplitude reduces to zero.

## CONTROLLER DESIGN

### Bifurcation Diagram

Adjusting the AC drive voltage  $V_{ac}$  shifts the entire frequency response curve in Figure 2, thus resulting in changes in the bifurcation points A and B. These shifts in A and B are graphically represented in Figure 3, which defines the “instability tongue” with the locus of the amplitude jump points. The right curve is the up-sweep bifurcation frequency (analogous to point B in Figure 2) showing the falling edge of the instability; the left curve is the down-sweep bifurcation frequency (point A). The DC voltage is fixed at 10 V.

The changes in the drive voltages modify the system’s effective spring constant, which affects the bending of the resonance curve and the regions where the system enters instability. In a typical nonlinear resonator, the drive voltage shapes the instability tongue. The tongue width

measured in frequency depends on the AC drive amplitude. The position of the tongue along the frequency axis is a strong function of the DC polarization voltage.

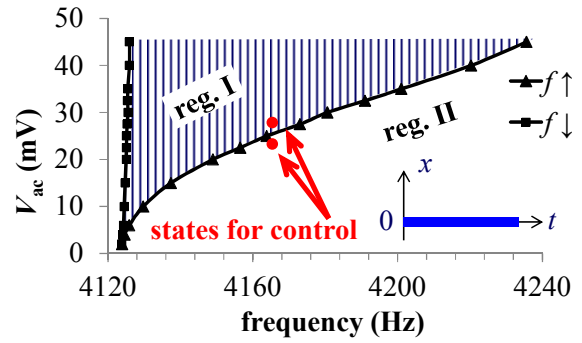


Figure 3: Measured bifurcation diagram of the regions I (“on” state) and II (“off” state).

The red dots in Figure 3 identify the states for a bi-state control loop. One of the states (“on” state) is inside the region I which has a large amplitude response; the other state (“off” state) resides in region II, outside of the tongue, representing a low amplitude response. The two states center around  $V_{ac} = 25\text{ mV}$  and have the same fixed frequency at the bifurcation frequency  $f_B$  for the  $V_{ac} = 25\text{ mV}$  setpoint. The two states are then on opposite sides of the bifurcation point in steady-state operation.

### Controller Schematic

The control loop is schematically shown in Figure 4. The control setpoint of the loop is chosen at point B in Figure 1. The AC drive frequency and the DC bias are fixed to values such that the system can be moved between instability and stability with appropriate bi-state values of AC amplitude  $|V_{ac}|$ . In the experiment, the DC bias voltage  $V_{dc,set} = 10\text{ V}$  and the AC drive frequency is  $f_B = 4167\text{ Hz}$ . The Duffing resonator is driven by  $V_{ac}$  whose amplitude and frequency are set by the pulse-width-modulator (PWM) output and the lock-in amplifier (LIA), respectively. A transimpedance amplifier followed by the LIA picks up the resonator velocity amplitude  $|v_{\tilde{x}}|$ . The loop tracks  $|v_{\tilde{x}}|$  to a fixed setpoint  $V_{thresh}$ . The error output is fed into a PID (proportional-integral-derivative) controller to generate the input signal to the PWM representing the pulse-train duty cycle. The output of the PWM generates the bi-state signal that sets the AC drive amplitude.

The  $V_{ac}$  is controlled by the feedback and rapidly turns the oscillation on and off at 300 kHz to achieve the servo at the maximum “on” point without turning off the resonator. This avoids the long ring-down transient needed to settle

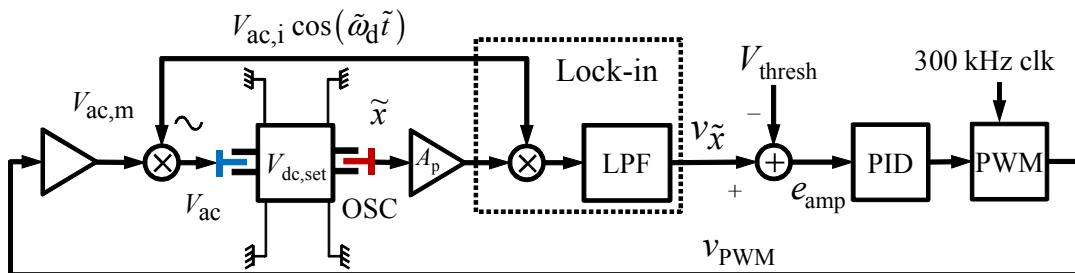


Figure 4: Block diagram of the bi-state Duffing controller with an SOI resonator as the plant and off-chip electronics.

from the “on” state to the “off” state. This resettling time is inversely proportional to the damping and is on the order of 1 s for the resonator operated under a vacuum of 22 mTorr.

## RESULTS

### Instability edge

A time-domain transient frequency chirp test is performed to explore the edge of the instability. The frequency is swept through the bifurcation frequency ( $f_B = 4167$  Hz). The initial swept frequency is backed off from the bifurcation frequency  $f_B$  so the jump can be observed. As the frequency approaches  $f_B$ , the oscillation amplitude drops from  $4.8 \mu\text{m}$  to a very small displacement. The displacement of  $1.8 \mu\text{m}$  seen in the “off” state of Figure 5 corresponds to a small voltage output (3.0 mV) from the capacitive pick-off circuit ( $A_p$  in Figure 4), which is due to the feedthrough from the  $V_{ac}$  drive to the capacitive sense comb.

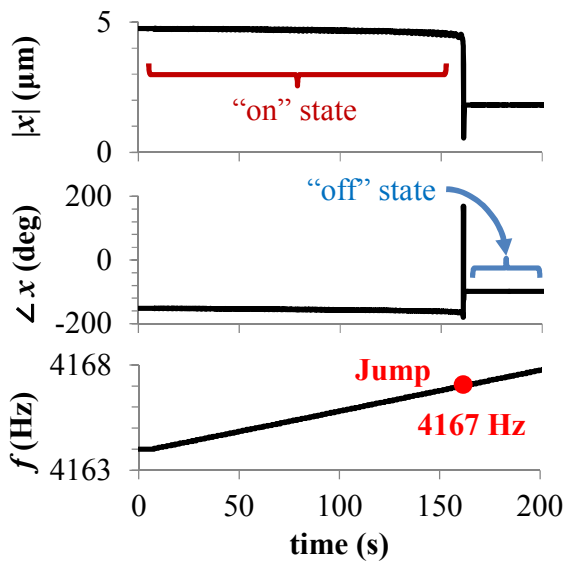


Figure 5: Turn-off transient of the Duffing resonator. The resonator is turned off when the frequency is swept beyond the bifurcation frequency at 4167 Hz.

### Turn-on Transients

Figure 6 is the turn-on transient of the closed-loop controller with an initial approaching phase. During region (1), the resonator is off. After (2), a sinusoidal voltage at 4123 Hz is applied to the resonator drive fingers, resulting in a step turn on of the displacement amplitude to a non-zero value due to the capacitive feedthrough. The choice of the initial frequency ensures the resonator is within its “off” state (to the left of point A in Figure 2). Region (3) is the necessary “approach” stage when the resonator is turned on to the maximum displacement operation point (point B in Figure 2) by increasing the drive frequency from 4123 Hz to 4167 Hz. The PID controller threshold  $V_{\text{thresh}}$  is set in (4) after reaching this maximum operation point, turning on the servo, after which time the PWM output rapidly changes between 0.3 V and 3.4 V, with duty cycle centered on 0.5. At (5), the servo is switched off by turning off  $V_{ac}$ . The phase is well-defined during the time the controller is on and loses track of the input  $V_{ac}$  when the controller is turned off.

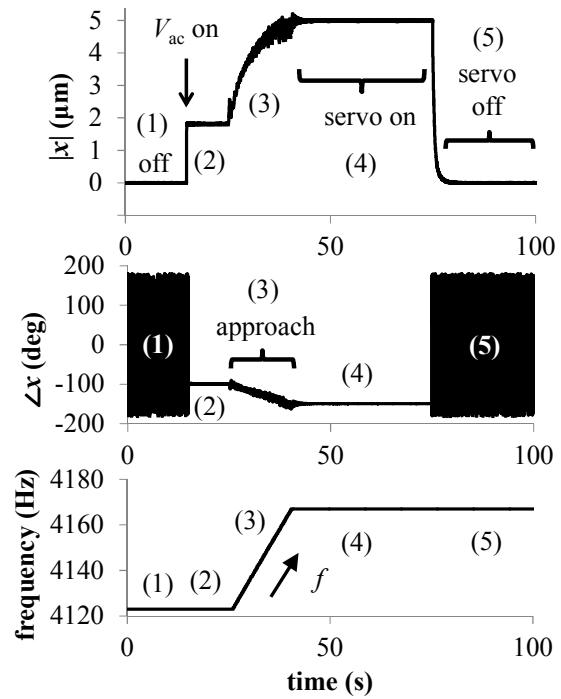


Figure 6: Turn-on transient of the bi-state control loop. The drive AC voltage is turned on at 15 s, followed by an approach phase when the frequency is increased from 4123 Hz to 4167 Hz. The controller is turned on afterwards. At 75 s, the controller is turned off by switching off  $V_{ac}$ .

### Off-State Dynamics

A detailed analysis of the dynamics on the edge of the bifurcation jump provides information on how fast the controller should switch between two states to guarantee successful recapturing of the “on” state. These “off-state” dynamics are characterized in Figure 7 and Figure 8.

In open-loop operation, a step change in  $V_{ac}$  is introduced from 25.6 mV to 24.1 mV, at which voltage the resonator is not fully in the off state but rather just starting to turn off.  $V_{ac}$  is then turned back to 25.6 mV after a prescribed amount of time  $\Gamma$ . When  $\Gamma$  is less than 394.6 ms, the Duffing resonance is successfully recaptured as presented in Figure 7. When  $\Gamma$  is larger than 395.0 ms, the resonance falls back to the “off” state. The critical off-state time  $\Gamma$  at which the resonance is on the edge of being recaptured is 394.6 ms.

For both figures prior to  $t = 0$  (point F), the system operates at its maximum “on” state. After point F, the resonator starts to turn off and provides the initial condition for later step turn-on (point N). At point N, the system exhibits a step response due to the step turn-on in the drive amplitude  $V_{ac}$ . Depending on the length of the “off-state” time (the time between points F and N), the system can either recover from the decreased amplitude (Figure 7) or completely turns off (Figure 8). The bi-state signal must operate at a rate much higher than the critical off-state time to avoid the ringing. The recapture dynamics in Figure 7 gauge the “slow time” (i.e. time scale that is much longer than the resonance period) behavior of the Duffing resonator and thus provide the root-locus information for later optimization of the PID coefficients.

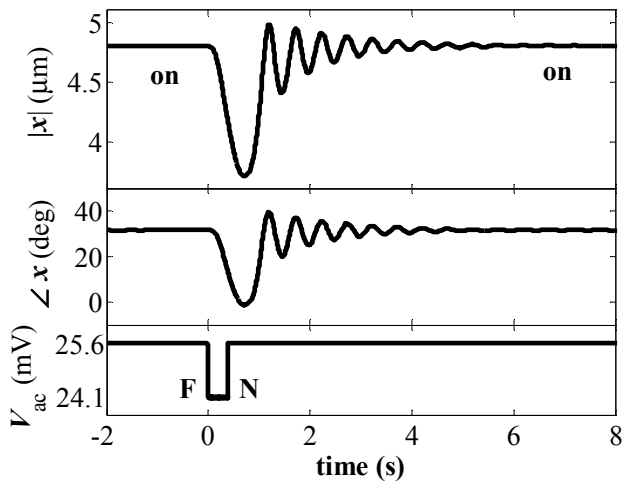


Figure 7: Successful recapture of the Duffing resonance by rapidly switching back to the “on” state. The critical off-state time is 394.6 ms.

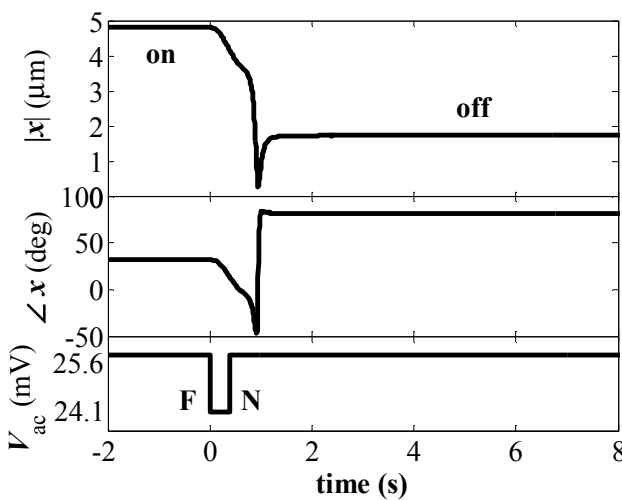


Figure 8: Turn-off of the Duffing resonance by increasing the off-state time beyond the critical off-state time. The turn-off time is 395.0 ms.

### Allan Variance

The Allan deviation of the normalized velocity amplitude  $|\bar{v}_x|$  is plotted in Figure 9 quantifying the stability of the loop. The control system output is sampled at 14.1 Hz for 14.2 hr. The vacuum level is maintained at

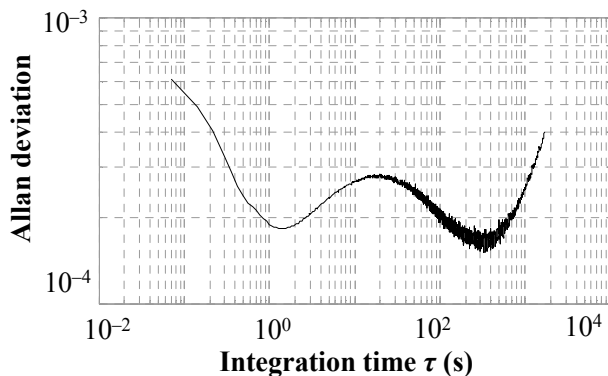


Figure 9: Allan deviation plot of the control system normalized velocity amplitude quantifying the stability.

22–24 mTorr. The output is normalized to the steady-state amplitude of 4.8  $\mu\text{m}$ . No temperature compensation is performed in the post-processing of the data due to the absence of a temperature sensor in the current vacuum testbench. The minimum detectable displacement is 0.7 nm at the integration time of 321 s. Further investigation of the two minimum peaking is slated.

### CONCLUSIONS

A bi-state bifurcation-based controller is successfully implemented to servo at the maximum “on” point prior to the bifurcation jump. The operation of the control loop is experimentally verified using a Duffing resonator fabricated in a 15  $\mu\text{m}$ -thick SOI process as the control plant. The close-loop control avoids the necessary setup and ring-down time that is required to settle between the “on” state and the “off” state. The bi-state servo technique provides a novel approach to track the bifurcation jump point at the maximum displacement amplitude, thus significantly increases the SNR compared to the state-of-the-art. The capability to servo on the edge of the instability promotes future implementation of an ultrasensitive bifurcation-based mass or stress detector.

### ACKNOWLEDGEMENTS

This work was sponsored by the National Science Foundation grant CNS 0941497. The authors thank E. Tatar for co-developing the fabrication process, and S. Santhanam and the CMU Nanofabrication Facility staff for their technical support.

### REFERENCES

- [1] A. Raman, A. K. Bajaj, and P. Davies, “On the slow transition across instabilities in non-linear dissipative systems,” *Journal of sound and vibration*, vol. 192, no. 4, pp. 835-865, 1996.
- [2] C. Guo, K. M. Shah, and G. K. Fedder, “Electrically driven CMOS-MEMS nonlinear parametric resonator design using a hierarchical MEMS circuit library,” in *Transducers '11*, June 5–9, 2011, pp.2402–2405.
- [3] C. Guo and G. K. Fedder, “Behavioral modeling and testing of a CMOS-MEMS parametric resonator governed by the nonlinear Mathieu equation,” in *the 25th Int. Conf. Micro Elec. Mech. Sys., (MEMS 2012)*, Paris, France, 29 Jan–2 Feb 2012, pp. 535–538.
- [4] C.B. Burgner, W.S. Snyders, K.L. Turner, “Control of MEMS on the edge of instability,” in *Transducers '11 Conference*, pp.1990–1993, June 5–9, 2011.
- [5] C.B. Burgner, L.A. Shaw, K.L. Turner, “A new method for resonant sensing based on noise in nonlinear MEMS,” in *the 25th Int. Conf. Micro Electro Mechanical Systems, (MEMS 2012)*, pp. 511–514, Paris, France, 29 Jan–2 Feb 2012.
- [6] C. Guo, E. Tatar, and G. K. Fedder, “Large-displacement parametric resonance using a shaped comb drive”, in *the 26th Int. Conf. Micro Electro Mechanical Systems (MEMS 2013)*, pp. 173–176, Taipei, Taiwan, 20 – 24 Jan 2013.

### CONTACT

\* Congzhong Guo, tel: 1-412-268-4403; czguo@cmu.edu